Optical attenuation correction in multispectral optoacoustic tomography with logarithm unmixing

X Luís Deán-Ben, Andreas Buehler, Vasilis Ntziachristos and Daniel Razansky *
Institute for Biological and Medical Imaging, Technical University of Munich and Helmholtz
Center Munich, Ingolstädter Landstraße 1, 85764 Neuherberg, Germany.

ABSTRACT

Quantification of extrinsically administered contrast agents in optoacoustic (photoacoustic) tomography is a challenging task, mainly due to spectrally-dependent contributions from absorbing background tissue chromophores leading to strong changes in the light fluence for different positions and wavelengths. Herein we present a procedure capable of self-calibrating light fluence variations for quantitative imaging of the distribution of photo-absorbing agents. The method makes use of a logarithmic representation of the images taken at different wavelengths assisted with a blind unmixing approach. It is shown that the serial expansion of the logarithm of an image contains a term representing the ratio between absorption of the probe of interest and other background components. Provided the background variations are not very high, this term can be isolated with an unmixing algorithm, so that the concentration of the probe can subsequently be resolved.

Keywords: Optoacoustic tomography, photoacoustic tomography, multispectral unmixing, optical attenuation

1. INTRODUCTION

Optoacoustic tomography (OAT) refers to a hybrid optical and ultrasonic imaging modality based on the photoacoustic effect.¹ The rich contrast of OAT stems from the optical absorption of light within biological tissues whereas spatial resolution is determined by the ultrasonic diffraction limit, being significantly better to what is normally achieved by optical diffusion imaging techniques at depths of several millimetres to centimetres in tissue.² The intrinsic absorption of light in tissues in the visible and near-infrared is mainly due to oxygenated and deoxygenated haemoglobin. Thereby, high-resolution anatomical or structural imaging can be achieved by reconstructing the background absorption within the sample.^{3–5} By taking measurements at several optical wavelengths, multi-spectral optoacoustic tomography (MSOT) is also capable of determining the blood oxygenation levels on a per-pixel basis.⁶ Furthermore, it has recently been shown that molecular targets having a specific wavelength-dependent absorption can be similarly resolved from the images at different wavelengths, making MSOT a promising technique for molecular imaging applications.^{7,8}

Molecular imaging implies monitoring a biological process by accurately determining the distribution of a biomarker targeting a certain pathway at the cellular and molecular level. In order for the biological characterization to be meaningful, the resulting image should represent a quantitative distribution of the concentration of the molecular agent. In principle, this can be achieved by MSOT as the optical absorption coefficient of a light absorbing substance is generally proportional to its concentration. However, in order to obtain a quantitative image of the distribution of the optical absorption coefficient, several challenging issues must be addressed. First, the optoacoustic tomographic reconstructions must be quantitative and free of artifacts. For this, an accurate reconstruction algorithm must be employed. Commonly used back-projection algorithms, although simple and fast, do not faithfully represent the light absorption distribution, so that it is preferable to use algorithms based on the numerical inversion of the analytical solution of the optoacoustic wave equation.

9-11 Additional artifacts may appear in the images due to various acoustic propagation effects 12-16 or the operational characteristics of the ultrasonic transducer, 17,18 so that the reconstruction algorithms must be modified accordingly if such effects introduce unwanted distortion in the images. Second, the optoacoustic signals are in fact proportional to the product of the optical absorption coefficient and the light fluence. The light fluence within biological tissues decreases strongly with depth due to optical attenuation, which is generally significantly higher as compared

*E-mail: dr@tum.de

to acoustic attenuation in the frequency range of standard optoacoustic tomographic systems.¹⁹ Consequently, it becomes important to remove the light fluence dependence from the optoacoustic images in order to obtain the light absorption coefficient distribution. Finally, a spectral unmixing procedure, which considers the images taken at different wavelengths, must be employed in order to isolate the biomarker of interest. For this, blind unmixing techniques have been shown experimentally to have a higher sensitivity,²⁰ which is of special importance for visualizing low concentrations of biomarkers.

In this work we present a procedure capable of self-calibrating light fluence variations for quantitative imaging of the distribution of an extrinsically-administered photo-absorbing agent (probe). The method makes use of a logarithmic representation of the images taken at different wavelengths and blind unmixing. Performance is tested with experimental measurements made on a tissue-mimicking phantom containing optical probes at different depths.

2. THEORY

Optoacoustic tomographic reconstructions represent the distribution of the absorbed optical energy $H(\mathbf{r}, \lambda)$ within a biological tissue for a given laser wavelength λ . Assuming a constant Grueneisen parameter, $H(\mathbf{r}, \lambda)$ in arbitrary units is given by¹

$$H(\mathbf{r}, \lambda) = U(\mathbf{r}, \lambda)\mu_a(\mathbf{r}, \lambda),$$
 (1)

where $U(\mathbf{r}, \lambda)$ is the light fluence distribution and $\mu_a(\mathbf{r}, \lambda)$ is the optical absorption coefficient. $\mu_a(\mathbf{r}, \lambda)$ is a linear combination of the optical absorption coefficients corresponding to the different absorbers, i.e.,

$$\mu_a(\mathbf{r}, \lambda) = \sum_i \mu_{ai}(\mathbf{r}, \lambda) = \sum_i \epsilon_i(\lambda)c_i(\mathbf{r}),$$
 (2)

with $\epsilon_i(\lambda)$ being the molar extinction coefficients and $c_i(r)$ the concentrations of the different absorbers.

In many applications, such as quantitative molecular imaging, it is essential to accurately determine the concentration of a biomarker used to selectively resolve a particular molecular target. Since the concentration of the biomarker is essentially proportional to its optical absorption coefficient, it is only necessary to determine the distribution of the optical absorption coefficient directly resulting from such biomarker. Yet, the optical absorption corresponding to the biomarker of interest must be first identified among other background absorbers present in the sample, which can be done by collecting multiwavelength data and applying multispectral unmixing techniques. However, optoacoustic reconstructions are also significantly affected by the light fluence distribution, which is wavelength dependent. Since photon fluence is heavily attenuated as a function of depth, the same probe embedded deep within tissue may thus appear weaker than the one closer to the illuminated surface. Thus, it is also essential to decouple the optical absorption coefficient from the light fluence. In many practical cases, the two problems cannot be solved simultaneously.

In this work, we investigate an unmixing procedure that allows obtaining images of the biomarker concentration not affected by the light fluence distribution. In the first step, Eq. 1 is rewritten as

$$H(\mathbf{r}, \lambda) = U(\mathbf{r}, \lambda)[\mu_{ac}(\mathbf{r}, \lambda) + \mu_{ab}(\mathbf{r}, \lambda)],$$
 (3)

where $\mu_{ac}(\mathbf{r}, \lambda)$ is the absorption coefficient of the photo-absorbing molecule(s) of interest and $\mu_{ab}(\mathbf{r}, \lambda)$ represents the absorption coefficient of the background. By taking the logarithm of Eq. 3, one obtains

$$\log[H(\mathbf{r},\lambda)] = \log[U(\mathbf{r},\lambda)] + \log[\mu_{ab}(\mathbf{r},\lambda)] + \log[\frac{\mu_{ac}(\mathbf{r},\lambda)}{\mu_{ab}(\mathbf{r},\lambda)} + 1]. \tag{4}$$

Taylor series expansion of the last term in Eq. 4 leads to

$$\log[H(\mathbf{r},\lambda)] = \log[U(\mathbf{r},\lambda)] + \log[\mu_{ab}(\mathbf{r},\lambda)] + \frac{\mu_{ac}(\mathbf{r},\lambda)}{\mu_{ab}(\mathbf{r},\lambda)} - \frac{1}{2} \left[\frac{\mu_{ac}(\mathbf{r},\lambda)}{\mu_{ab}(\mathbf{r},\lambda)}\right]^2 + \dots$$
 (5)

The component $\mu_{ac}(\mathbf{r}, \lambda)/\mu_{ab}(\mathbf{r}, \lambda)$ can in principle be unmixed from Eq. 5 provided its variation with respect to the optical wavelength is different as compared to variations of the other terms. In that case, if the background absorption is approximately constant, the resulting image will be proportional to $\mu_{ac}(\mathbf{r}, \lambda)$.

This procedure however relies on the capability of the unmixing algorithm employed to isolate the term $\mu_{ac}(\mathbf{r},\lambda)/\mu_{ab}(\mathbf{r},\lambda)$ from $\log[H(\mathbf{r},\lambda)]$, which may not always be feasible. In biological tissues, the background absorption in the near infrared is mainly due to oxygenated and deoxygenated haemoglobin, so that the spectral dependence of $\mu_{ac}(\mathbf{r},\lambda)/\mu_{ab}(\mathbf{r},\lambda)$ depends on the oxygenation level of blood. As a result, the given component may be incorrectly unmixed if the variation of $\mu_{ab}(\mathbf{r},\lambda)$ with the wavelength differs for regions having different background. Furthermore, if $\mu_{ac}(\mathbf{r},\lambda) >> \mu_{ab}(\mathbf{r},\lambda)$, the higher order terms of the series expansion become significant, which may hamper the unmixing of $\mu_{ac}(\mathbf{r},\lambda)/\mu_{ab}(\mathbf{r},\lambda)$. The unmixing may also be inconvenient if the biomarker of interest is located in the blood vessels, as in that case $\mu_{ab}(\mathbf{r},\lambda)$ has a high value, so that the distribution of the optical absorption coefficient cannot be accurately imaged by considering the term $\mu_{ac}(\mathbf{r},\lambda)/\mu_{ab}(\mathbf{r},\lambda)$.

Various unmixing methods can potentially be employed to isolate the term $\mu_{ac}(\mathbf{r},\lambda)/\mu_{ab}(\mathbf{r},\lambda)$ in Eq. 5. The simplest method consists in subtracting the values of $\log[H(\mathbf{r},\lambda)]$ for two different wavelengths corresponding to high and low absorption of the biomarker of interest whereas background absorption remains approximately the same for these wavelengths. Higher sensitivity and accuracy can however be achieved with other unmixing methods that make use of higher number of optical wavelengths. In this work, we use a blind unmixing procedure based on a combination of principal component analysis (PCA) and independent component analysis (ICA) described in detail in Ref. 20. Thereby, a set of images corresponding to n optical wavelengths are first processed with the PCA algorithm for dimension reduction. Then, the first m components are processed with the ICA algorithm, yielding both the spectral signature and the distribution map of the chromophores present in the sample.

3. MATERIALS AND METHODS

Experimental measurements were done with a real-time optoacoustic tomographic system described in Ref. 21. Basically, a short-pulsed laser with a tunable wavelength was used as illumination source. The output beam was guided by means of a fiber bundle to create a ring-type illumination on the surface of the sample. The generated ultrasonic waves were detected with a phased-array transducer consisting of 64 elements covering an angle of 172°. Each element of the array is cylindrically focused with a focal length of 40 mm and a central frequency of 5 MHz. The signals were averaged 20 times and a band-pass filter with cut-off frequencies 0.1 and 7 MHz was applied. Image reconstruction was performed with a model-based algorithm described in Ref. 22.

A tissue-mimicking agar phantom was imaged. Black India ink and Intralipid were added to the agar solution in order to simulate the background optical absorption and optical scattering of biological tissues, namely $\mu_a = 0.2 \text{ cm}^{-1}$ and $\mu'_s = 10 \text{ cm}^{-1}$. Two insertions with AlexaFluor 750 (AF750) and two insertions with gold nanorods (GN) were included at different depths within the phantom. The peak absorption of these photo-agents was approximately $\mu_a = 1 \text{ cm}^{-1}$ as measured with a spectrometer. Black ink was also included in all four insertions with absorption equal to the background. The phantom was imaged for 21 equally-spaced wavelengths ranging from 700 to 900 nm.

4. RESULTS

The optoacoustic tomographic reconstructions corresponding to the experiment described in section 3 were unmixed by applying the combination of the PCA and ICA algorithms to the original images and to the logarithm of the images. The results are displayed in Fig. 1. Figs. 1a and 1b showcase, respectively, the tomographic reconstructions obtained at 750 nm (approximately the absorption peak of AF750) and at 780 nm (approximately the absorption peak of GN). The unmixed images and the spectra obtained with standard blind unmixing corresponding to AF750 and GN are shown in Figs. 1c and 1d respectively. The corresponding images and spectra retrieved with the procedure described in this work are displayed, respectively, in Figs. 1e and 1f. Figs. 1g and 1h showcase the profiles A-A and B-B (marked in Figs. 1a and 1b) for the unmixed images corresponding to AF750 and GN. It is shown that the reduction of amplitude due to light attenuation present in the first case is corrected if the procedure presented herein is used.

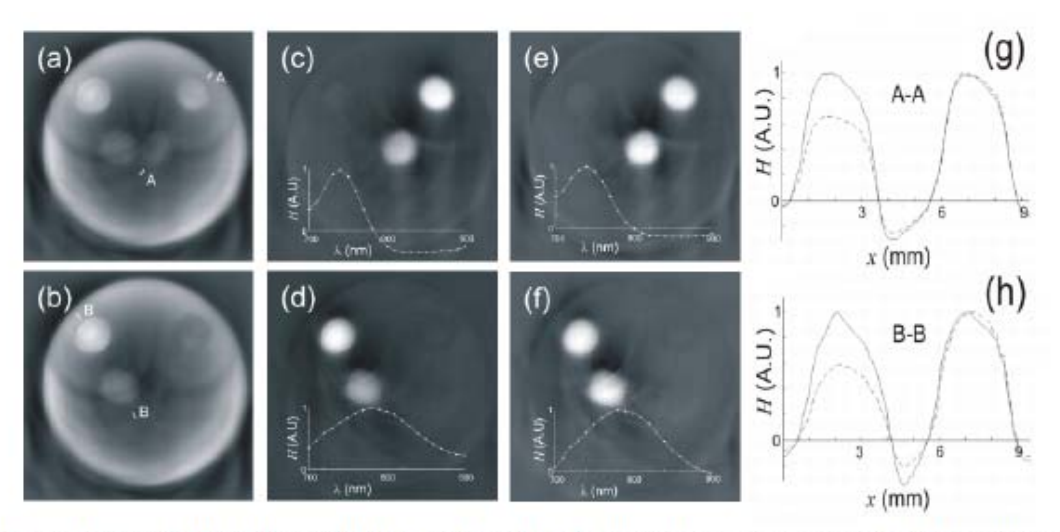


Figure 1. Unmixing results of AlexaFluor 750 (first row) and gold nanoparticles (second row) for the phantom experiment.

(a)-(b) Tomographic optoacoustic reconstructions for 750 nm and 780 nm respectively. (c)-(d) Standard unmixing. (e)-(f) Logarithmic unmixing. (g)-(h) Profiles A-A and B-B indicated in (a) and (b) respectively for standard unmixing (dashed lines) and logarithmic unmixing (continuous lines).

5. DISCUSSION AND CONCLUSIONS

The experimental results show that the suggested blind logarithmic unmixing method presented in this work is able to correct for the light attenuation effects in the unmixed images corresponding to the absorbed energy of a specific photo-absorbing agent. The method relies on the unmixing algorithm to retrieve the desired component of the logarithm of the images, while the rendered images correspond to the ratio of the absorption coefficient of the probe and the absorption coefficient of the background. As a result, the efficiency of the correction is still affected by several limiting factors. If, for instance, the wavelength-dependent absorption of the background varies significantly for different regions within the sample (which in practice relates to strong blood oxygenation changes), the spectral signature of the term $\mu_{ac}(\mathbf{r}, \lambda)/\mu_{ab}(\mathbf{r}, \lambda)$ would also become space-dependent. Consequently, it may be difficult to isolate this term with the unmixing algorithm. The unmixing algorithm may also render inaccurate results in case the absorption due to the component of interest is much higher as compared to the background absorption, as in that case the higher order terms of the series expansion in Eq. 5 may also have a significant contribution. For an optical absorption of the probe in the order of the background absorption or lower, which is desirable in practice, these inaccuracies are not significant.

In conclusion, the good performance of the self-calibration optoacoustic unmixing method presented in this work anticipates its convenience in applications requiring quantitative molecular imaging, as the spatial distribution of the absorption coefficient is proportional to the spatial distribution of the concentration of an external agent injected in the biological specimen to be imaged.

ACKNOWLEDGMENTS

Daniel Razansky acknowledges support from the German Research Foundation (DFG) Research Grant (RA 1848/1) and the ERC Starting Independent Researcher Grant. Vasilis Ntziachristos acknowledges support from the ERC Senior Investigator Award and the Medizin Technik BMBF award for excellence in medical innovation.

REFERENCES

- Wang, L. V., ed., [Photoacoustic imaging and spectroscopy], CRC Press, Boca Raton (USA) (2009).
- [2] Wang, L. V. and Wu, H. I., [Biomedical Optics: Principles and Imaging], John Wiley & Sons, New Jersey (USA) (2007).
- [3] Brecht, H. P., Su, R., Fronheiser, M., Ermilov, S. A., Conjusteau, A., and Oraevsky, A. A., "Whole-body three-dimensional optoacoustic tomography system for small animals," *Journal of Biomedical Optics* 14(6), 064007 (2009).

- [4] Laufer, J., Zhang, E., Raivich, G., and Beard, P., "Three-dimensional noninvasive imaging of the vasculature in the mouse brain using a high resolution photoacoustic scanner," Applied Optics 48(10), D299–D306 (2009).
- [5] Ma, R., Distel, M., Deán-Ben, X. L., Ntziachristos, V., and Razansky, D., "Non-invasive whole-body imaging of adult zebrafish with optoacoustic tomography," *Physics in Medicine and Biology* 57(22), 7227–7237 (2012).
- [6] Zhang, H. F., Maslov, K., Stoica, G., and Wang, L. V., "Functional photoacoustic microscopy for high-resolution and noninvasive in vivo imaging," Nature Biotechnology 24, 848–851 (2006).
- [7] Razansky, D., Distel, M., Vinegoni, C., Ma, R., Perrimon, N., Koster, R. W., and Ntziachristos, V., "Multispectral opto-acoustic tomography of deep-seated fluorescent proteins in vivo," *Nature Photonics* 3(7), 412–417 (2009).
- [8] Ntziachristos, V. and Razansky, D., "Molecular imaging by means of multispectral optoacoustic tomography (msot)," Chemical Reviews 110(5), 2783–2794 (2010).
- [9] Paltauf, G., Viator, J. A., Prahl, S. A., and Jacques, S. L., "Iterative reconstruction algorithm for optoacoustic imaging," Journal of the Acoustical Society of America 112(4), 1536–1544 (2002).
- [10] Rosenthal, A., Razansky, D., and Ntziachristos, V., "Fast semi-analytical model-based acoustic inversion for quantitative optoacoustic tomography," IEEE Transactions on Medical Imaging 29(6), 1275–1283 (2010).
- [11] Deán-Ben, X. L., Buehler, A., Ntziachristos, V., and Razansky, D., "Accurate model-based reconstruction algorithm for three-dimensional optoacoustic tomography," *IEEE Transactions on Medical Imaging* 31(10), 1922–1928 (2012).
- [12] Xu, Y. and Wang, L. V., "Effects of acoustic heterogeneity in breast thermoacoustic tomography," IEEE Transactions on Ultrasonics, Ferroelectrics and Frequency Control 50(9), 1134–1146 (2003).
- [13] Deán-Ben, X. L., Ma, R., Razansky, D., and Ntziachristos, V., "Statistical approach for optoacoustic image reconstruction in the presence of strong acoustic heterogeneities," *IEEE Transactions on Medical Imaging* 30(2), 401–408 (2011).
- [14] Deán-Ben, X. L., Ntziachristos, V., and Razansky, D., "Statistical optoacoustic image reconstruction using a-priori knowledge on the location of acoustic distortions," Applied Physics Letters 98(17), 171110 (2011).
- [15] Modgil, D., Anastasio, M. A., and Riviere, P. J. L., "Image reconstruction in photoacoustic tomography with variable speed of sound using a higher-order geometrical acoustics approximation," *Journal of Biomedical Optics* 15(2), 021308 (2010).
- [16] Deán-Ben, X. L., Ntziachristos, V., and Razansky, D., "Artefact reduction in optoacoustic tomographic imaging by estimating the distribution of acoustic scatterers," *Journal of Biomedical Optics* 17(11), 110504 (2012).
- [17] Wang, K., Ermilov, S. A., Su, R., Brecht, H. P., and Oraevsky, A. A., "An imaging model incorporating ultrasonic transducer properties for three-dimensional optoacoustic tomography," *IEEE Transactions on Medical Imaging* 30(2), 203–214 (2011).
- [18] Rosenthal, A., Ntziachristos, V., and Razansky, D., "Model-based optoacoustic inversion with arbitraryshape detectors," Medical Physics 38(7), 4285–4295 (2011).
- [19] Deán-Ben, X. L., Razansky, D., and Ntziachristos, V., "The effects of acoustic attenuation in optoacoustic signals," Physics in Medicine and Biology 56(18), 6129-6148 (2011).
- [20] Glatz, J., Deliolanis, N. C., Buehler, A., Razansky, D., and Ntziachristos, V., "Blind source unmixing in multi-spectral optoacoustic tomography," Optics Express 19(4), 3175–3184 (2011).
- [21] Buehler, A., Herzog, E., Razansky, D., and Ntziachristos, V., "Video rate optoacoustic tomography of mouse kidney perfusion," Optics Letters 35(14), 2475–2477 (2010).
- [22] Deán-Ben, X. L., Nziachristos, V., and Razansky, D., "Acceleration of optoacoustic model-based reconstruction using angular image discretization," *IEEE Transactions on medical imaging* 31(5), 1154–1162 (2012).